

Design and Simulation of a New Topology of Single-Phase Stand-Alone Solar Inverters by Sinusoidal Duty Cycle Modulation

Gabriel Roméo Tobajio Haoudou¹, Arnaud Biyobo Obono², Léandre .N. Nneme³

^{1,2,3}Research Laboratory of Computer Science Engineering and Automation

Doctorate Training Unit for Engineering Sciences

Doctorate School for Pure and Applied Sciences

ENSET, University of Douala

Douala, Cameroon

Email: rtobajio@yahoo.fr

Abstract:

This paper focuses on the modeling and virtual simulation of a closed-loop photovoltaic single-phase inverter with characteristics: 230V-50Hz, apparent power 1KVA, equipped with a new robust control system by sinusoidal duty cycle modulation of modulation frequency 25 kHz. It follows on from work on the open-loop virtual simulation of a photovoltaic inverter using the same control principle. The duty cycle modulation used in this work present compared to the most widespread control strategy in its first approximation (PWM control technique): Low hardware complexity, A variable modulation frequency/period, A modulation topology with feedback. This new structure controlled by sinusoidal duty cycle modulation, equipped with PI controllers and the technique of maximum power disturb & observe (SPMP P&O); allows controlling the output current and voltage quantities of the PV inverter. The results obtained in the MATLAB / Simulink software made it possible to demonstrate a real reduction in the oscillations of the output voltage despite the strong stress of the variation of the load.

Keywords— Single Phase Inverter, Photovoltaic, Sinusoidal duty cycle Modulation, MPPT P&O, Robust Controller, Closed Loop, Virtual Simulation.

I. INTRODUCTION

Inverters are converters that transform DC/voltage into AC/voltage, are widely used in industrial applications. Some applications include: AC motor speed control, induction heating, emergency power supplies, uninterrupted power supplies [1], [2], [3], etc. In most of these applications, they are driven by the pulse width modulation control technique. The latter has under gone several evolutions from classical PWM to advanced PWM techniques [4], [5].

Although this is the most widely used control strategy, its basic structure is subjected to certain weaknesses such as: the complexity of the triangular modulation clock, the open-loop control

topology, the constant modulation frequency, etc. However, the new PWM technique has been developed to provide control of the system.

More so, the new technique of duty cycle modulation (DCM), developed since 2005, has proven to have sufficient advantages to compete with existing classical modulation techniques[11],[13]: It has become a versatile modulation technique, with the following advantages: minimal implementation cost, low hardware complexity, variable modulation frequency (period), with the implication of a harmonic spectrum with low high-frequency harmonic components, minimal digital processing complexity, feedback modulation topology, with the consequence of more robustness to

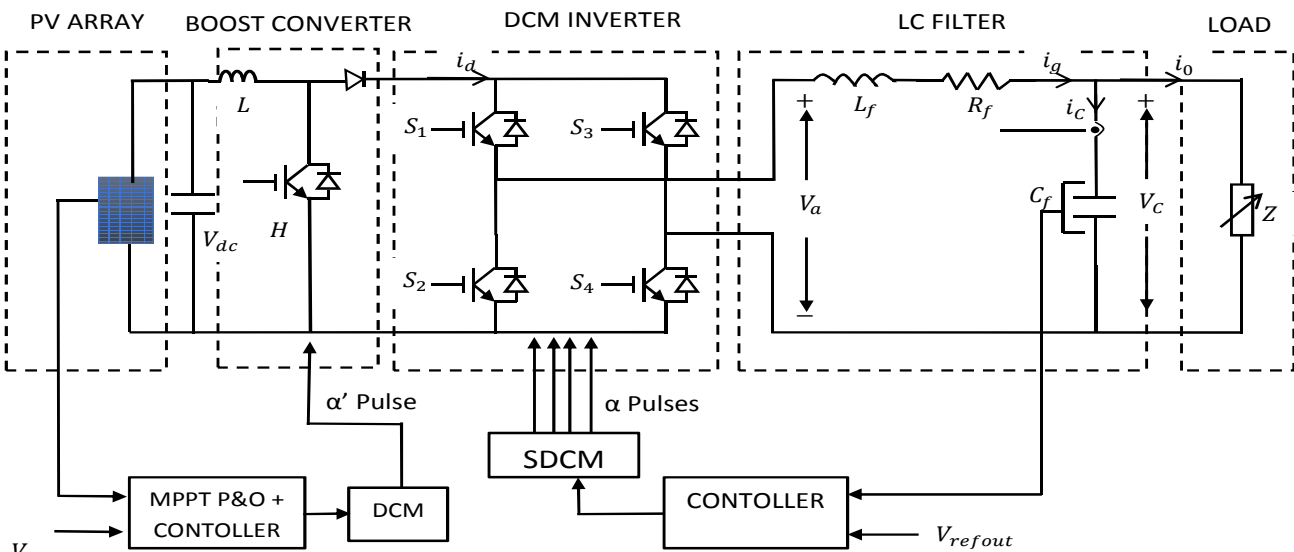
disturbances and optimal quality in a wide variety of systems [6],[7] [8], [9], [10], [11], [12], [13], [14], [15], [16], [17], [18], [19], [20].

In addition, a review proposed in 2018 [7], summarises all the fields explored so far by the DCM, such as signal processing [8], [9], [10] (analog-to-digital conversion/digital-to-analog conversion), power electronics (Buck, Buck-Boost and Boost chopper control) [16], [17], [18], [19], signal transmission and acquisition [20],[21], on the performance of industrial electronics and instrumentation processes driven by duty cycle modulators (DCM) [7]. In this review, it is clearly stated that the duty cycle modulator applied in the field of DC/AC conversion represents only 6% of the work that can be done in this field of power electronics. This rate represents the work on the control and implementation of a single-phase PV open-loop inverter by sinusoidal duty cycle modulation [15]. This study then focuses on the study and virtual simulation of a single-phase PV inverter in a closed-loop. It corrects the weaknesses observed during the open-loop study [15]. Indeed, in closed-loop, we observe robustness to disturbances, a stable output voltage despite load variations, and an improvement of the dynamic performance of the system which makes the single-phase PV inverter with sinusoidal duty cycle modulation control more efficient.

II. METHODS AND TOOLS

A. General Architecture Of The New Hybrid Single-Phase Inverter Prototype With Sinusoidal Duty Cycle

Figure 1 below shows the general architecture of the proposed new duty cycle modulated photovoltaic inverter prototype.



B. Photovoltaic Panels

The main components of the photovoltaic cell are semiconductor materials. Under the effect of light rays falling on a photovoltaic cell, it transforms them directly into electrical energy [11]. The photovoltaic panels constituting the photovoltaic field presented above are those of SUNTECH POWER STP 320-24-Ve, Consisting of 04 strings of 10 PV

C. Maximum Power Tracking Module (MPPT module)

For the PV array to deliver its maximum power at each moment, a maximum power tracking algorithm (MPPT P&O) is used, due to its simplicity and ease of implementation compared to other techniques [24].

The voltage and current of the PV array are the inputs to the algorithm, and the pulses generated by the assembly (duty cycle modulator + MPPT algorithm + PI controller) are used to control the duty cycle α' of the Boost Converter.

D. Boost Chopper

The role of this boost chopper is to raise the voltage value at the output of the PV field, which must be sufficient to charge the storage battery [22], [23], [24], and power the MOSFET inverter bridge. In this work, the voltage at the input of the bridge is $80V \pm 5\%$ and a current of $13.7A \pm 1\%$ corresponding to a voltage at the output of the Boost chopper of 160V under a duty cycle $\alpha'=0.5$. The structure of the chopper used is shown in Figure 2 below.

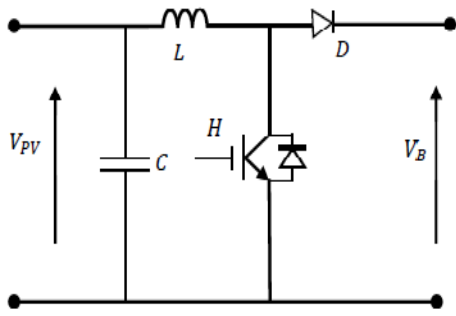


Fig. 2. Structure of the BOOST chopper

The voltage and current at the output are related to those at the input by the following relationships:

$$\begin{cases} V_B = \frac{V_{PV}}{1-\alpha'} \Rightarrow V_s = \frac{80}{1-0,5} = 160 \Rightarrow V_s = 160V & (1) \\ I_s = (1-\alpha')I_{PV} \Rightarrow I_s = (1-0,5)13,70=6,80 \Rightarrow I_s = 6,80A \end{cases}$$

The inductors and capacitors of the BOOST structure in figure 2 above are thus sized as follows:

$$\begin{cases} C \geq \frac{\alpha'(1-\alpha')I_e}{f\Delta v_s} \Rightarrow C \geq \frac{0,5(1-0,5)13,70}{25 \times 10^3 \times 5} = 26.10^{-6} \Rightarrow C \geq 26\mu F \\ L \geq \frac{\alpha'V_e}{f\Delta i} \Rightarrow L \geq \frac{0,5 \times 80}{25 \times 10^3 \times 0,1370} \Rightarrow L \geq 11,678mH \end{cases} \quad (2)$$

E. Storage Battery

The main purpose of the battery bank is to store the additional electrical energy generated by the solar PV system and supply it to the load whenever the PV system is unavailable (bad weather, maintenance,...). The nominal voltage is 7.2V and the full load at about 8V, so to store all the 80V, 3 strings of about 10 8V batteries are needed. For a total nominal capacity of (4.8835x3= 14, 6505Ah) and its autonomy is 2Hours04Min, which means that the battery system can supply the load for more than two hours exactly if the PV system is out of service.

F. Duty Cycle Modulator

The duty cycle modulator shown in Figure 3 by its Simulink numerical model is a negative resistance controlled oscillator whose operating principle is based on charging and discharging the capacitor under a time constant of τ [7]. The resulting voltage is then compared to a sinusoidal voltage (This Simulink model, which represents the information flow carried by the duty cycle modulator, is characterized by the following parameters:

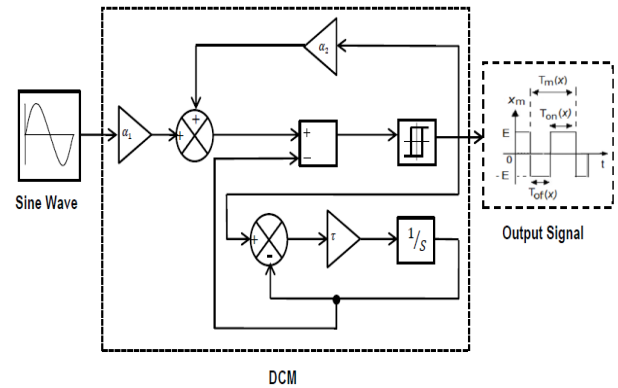


Fig 3: Simulink structure of the duty cycle modulator

This Simulink model, which represents the (I)flow of information conveyed by the duty cycle modulator, is characterized by the following parameters:

$$R_1 = 10K\Omega; \quad R_2 = 8,2K\Omega; \quad C = 1,6nF; \quad E = 12V$$

$$\begin{cases} \alpha_1 = \frac{R_1}{R_1 + R_2} \Rightarrow \alpha_1 = \frac{10}{10 + 8,2} \Rightarrow \alpha_1 = 0,5495 \\ \alpha_2 = 1 - \alpha_1 \Rightarrow \alpha_2 = 1 - 0,5495 \Rightarrow \alpha_2 = 0,4505 \\ f_m(0) = \frac{1}{R_1 C \ln\left(2 \times \frac{R_1}{R_2} + 1\right)} \Rightarrow f_m(0) = 25KHz & (3) \\ \tau = R_1 C \Rightarrow \tau = 16\mu s \end{cases}$$

On the basis of research published in the literature, let us recall that an DCM signal noted $x_m(t)$ and its characteristic quantities noted $R_m(x(t)) =$ duty cycle, $T_{of}(x(t))=$ positive pulse duration, $T_m(x(t))=$ modulation period, are described by the relations (4), available in [7] , [11] .

$$\begin{cases} R_m(x(t)) = \frac{T_{on}(x(t))}{T_m(x(t))} \\ \text{with} \\ T_{on}(x(t)) = \tau \ln\left(\frac{(1-\alpha)x - (1+\alpha)E}{(1-\alpha)x + (\alpha-1)E}\right) \\ T_m(x(t)) = \tau \ln\left(\frac{((1-\alpha)x)^2 - ((1+\alpha)E)^2}{((1-\alpha)x)^2 + ((\alpha-1)E)^2}\right) \end{cases} \quad (4)$$

The exact analytical expression of the modulation duty cycle $R_m(x(t))$, originally established in [6], is strongly non-linear in x. For this reason, it has been proven that there is an excellent linear approximation from the point of view of accuracy and modulating range by a 1st order Taylor expansion. Relation (5) corresponds to the linearized model defined in [11].

$$\begin{cases} R_m(x(t)) = P_m \cdot x(t) + \frac{1}{2} \quad \text{with} \\ P_m = \frac{\alpha_1 \cdot \alpha_2}{E(1 - \alpha_1^2)} \\ \log\left(\frac{1 + \alpha_1}{1 - \alpha_1}\right) \end{cases} \quad (5)$$

G. Mosfet Switches

The electronic switches chosen here are MOS switches of the IFR type, because of their operation at very high frequencies. They operate by alternately switching the switch pairs (S1, S4) and (S2, S3) at a frequency. These switches have the following characteristics: Ron=0,1Ω, Rd=0,01Ω, and a control signal of 5V; they are driven by sinusoidal duty cycle modulation α=0.54.

H. Frequency analysis

As previously mentioned in the open-loop study [15], the frequency analysis leads us to the bode diagram, whose amplitude and phase are given in figure 4 below

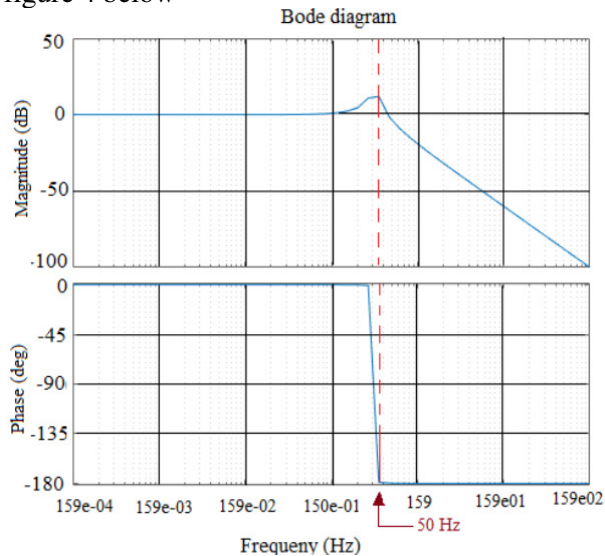


Fig 4: Bode diagram [15].

III. RESULTS AND DISCUSSIONS

A. Virtual Simulation Platform and Structure

The Simulink environment of Matlab is the platform used to perform the virtual simulations on the inverter prototype presented in this work.

This diagram indicates that the filter is a second-order low-pass type with a cut-off frequency and a passband, This will remove frequency harmonics.

The general structure of the new DC/AC conversion system using duty cycle modulation is composed of a power part and a control part and is given in Figure 5 below [26].

B. Technical Characteristics of the Elements Used for the Simulation

TABLE I
SUMMARY OF SIMULATION PARAMETERS

Elements	Characteristics
SDCM	$f_m(0)=25\text{Khz}$; $u_{\max}=2\text{V}$; $E=\pm 12\text{V}$; $\alpha = 0,5$
PV	$T = 25^\circ\text{C}$; $I_{\text{ro}} = 1000\text{W} / \text{m}^2$; $U_{\text{PV}} = 80\text{V}$
Boost chopper	$U_e = 80\text{V}$; $\alpha' = 0.5$; $U_s = 160\text{V}$
Battery bank	$Q = 14,6505\text{Ah}$; 02heures
Condensers	$C_1 = 75\mu\text{F}$; $C_2 = 150\mu\text{F}$
IRF Mosfet	$U^{cde} = 5\text{V}$; $f^{cde} = 25\text{khz}$
LC Filter	$r_f = 200\text{m}\Omega$; $L_f = 150\text{mH}$ et $C_f = 66\mu\text{F}$;
PI Controller	Voltage controller $K_p = 0,33$; $K_1 = 5$; Current controller $K_p = 1000$; $K_1 = 1333,33$

C. Current and Voltage at the PV Array Output

The current and voltage versus time characteristics at the output of the PV array are shown in Figure 7 below. It can be seen that the PV array delivers a constant current of 13.7A at a constant DC voltage of 80V.

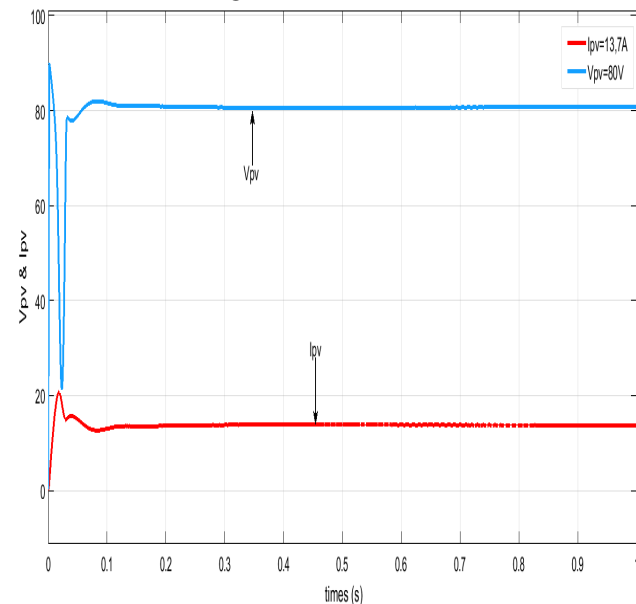


Fig.7. PV array current and voltage

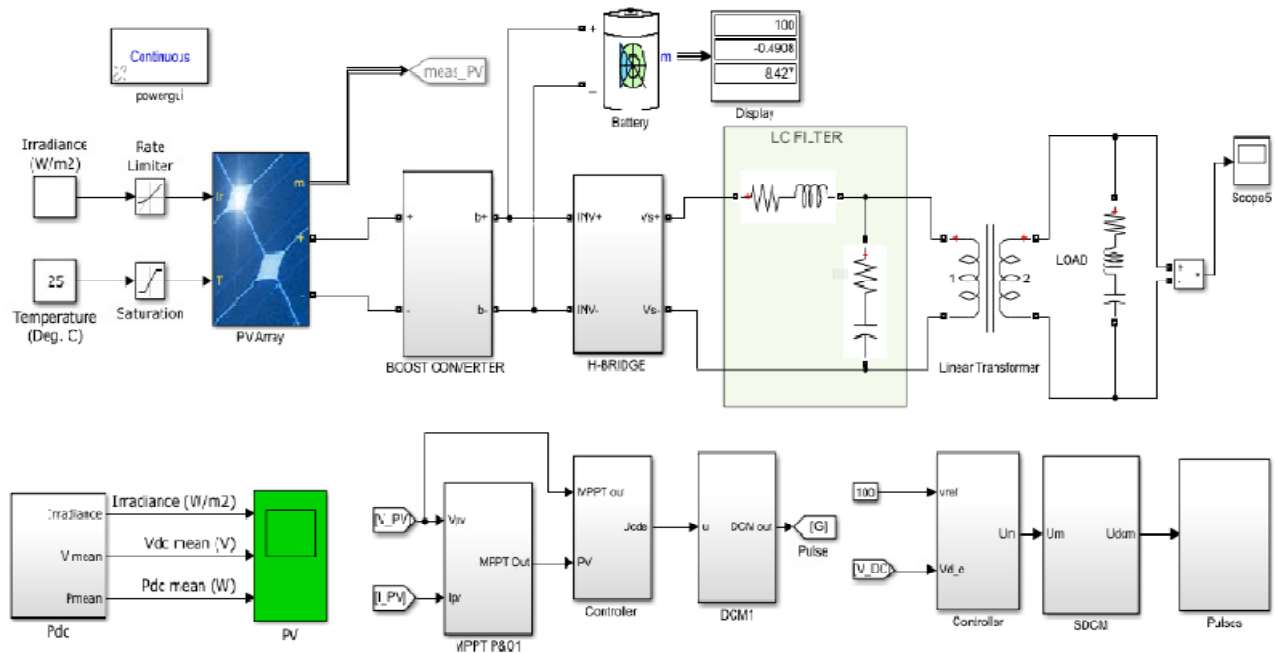


Fig. 5. Simulink structure of the PV stand-alone inverter with DCM control

D. PV Panel Power

The photovoltaic field consists of 4 photovoltaic panels of which one set, in two series and two in parallel, develops a constant continuous power of PPV=1,108KW. The characteristic in figure8 below represents the evolution of this power as a function of time. It is easy to see that after a transitory phase, this power stabilizes around the value indicated above.

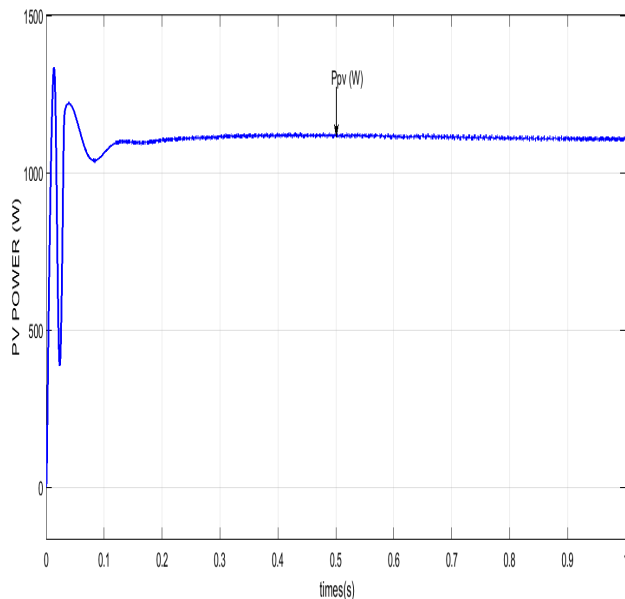


Fig.8. PV Array Power

E. Boost Chopper Output Voltage

The desired voltage at the input of the bridge is 160V corresponding to a voltage at the input of the boost chopper of 80V under a duty cycle $\alpha=0,5$. It can be seen from the figure 9 below that the output voltage of the parallel chopper rises and stabilizes at the output value of 160V.

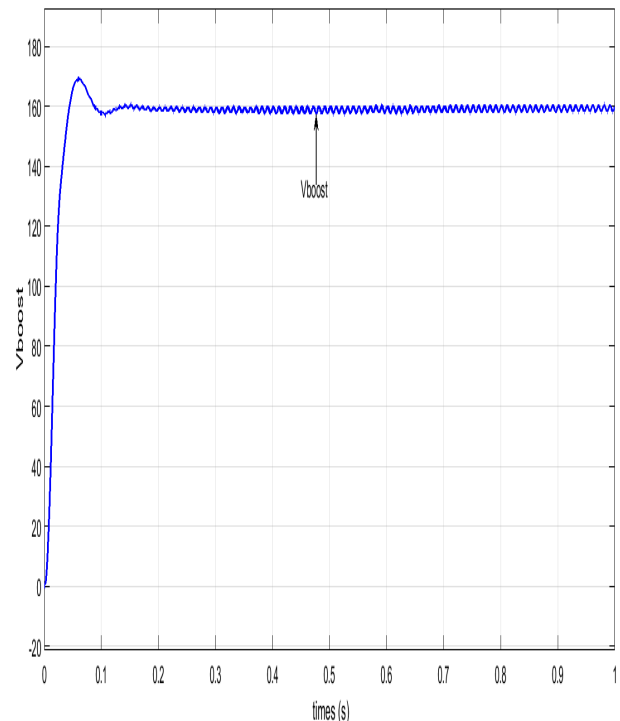


Fig.9. Voltage at the output of the boost chopper

F. Inverter Output Voltage

The output voltage of the H-bridge Mosfet is a rectangular AC voltage. It can be seen that the frequency of this inverter output signal is that of the power semiconductor switch control and its amplitude is that of the boost chopper output signal:

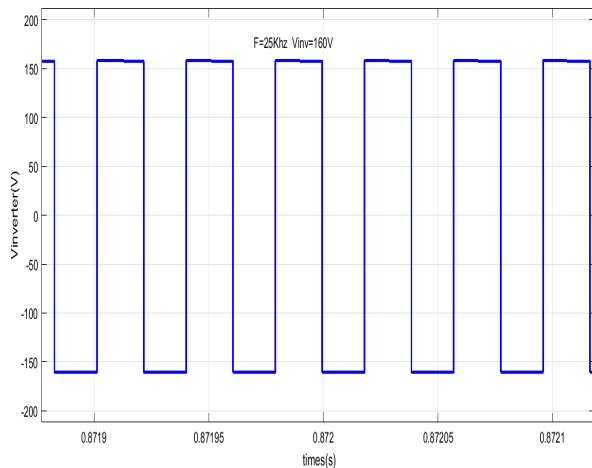


Fig.10. Inverter output voltage

G. Harmonic Spectrum of the Inverter Output Voltage

Figure 11 below shows the evolution of the harmonics in the steady-state signal. It can be seen that the rate of harmonic distortion is very disastrous, i.e. an overall rate of THD=201,18%.

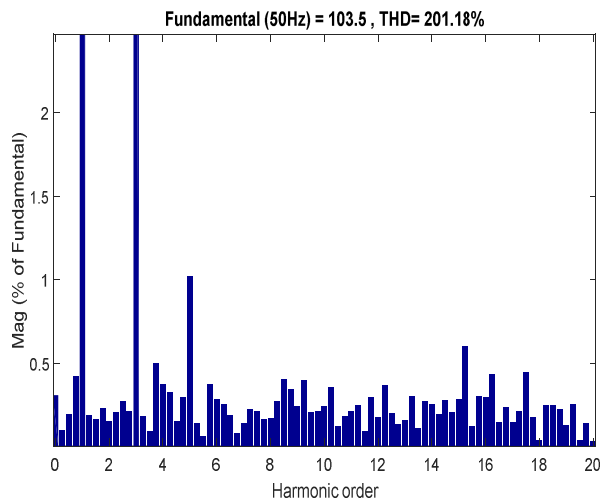


Fig.11. Harmonic spectrum of the inverter output voltage

H. Inverter Output Current

Figure 12 shows the sinusoidal alternating current available at the output of the inverter. It has amplitude of about 7A and a frequency of 50Hz.

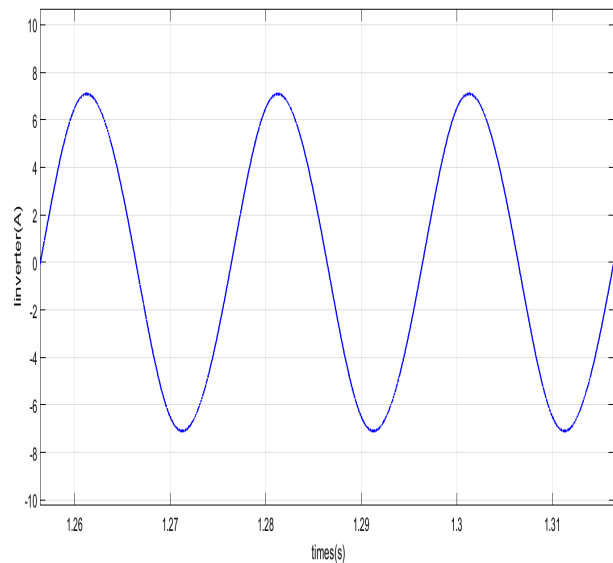


Fig.12. Inverter output current

I. Harmonic Spectrum of the PV Inverter Output Current

It can be seen that the overall current harmonic distortion at the output of the inverter is 1,16% THD acceptable according to EN50160.

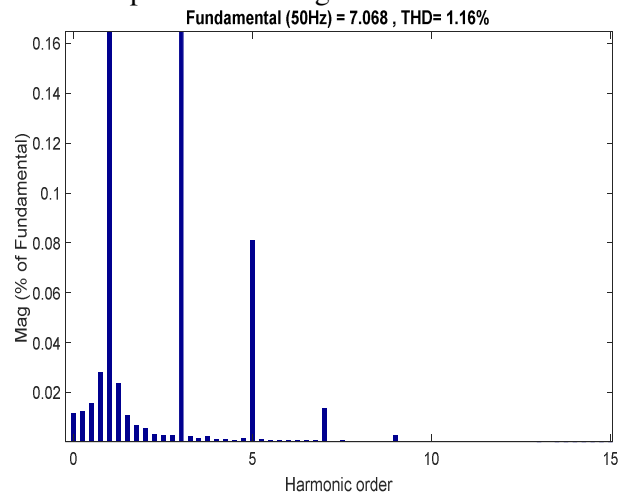


Fig13. Harmonic spectrum of the inverter output current

K. Voltage at the load terminals

The output voltage of the inverter or voltage at the load is alternating and sinusoidal. It represents the fundamental of the rectangular signal at the output of the bridge after passing through the filter. This sinusoidal voltage is the one that will be applied to the output of the inverter. This sinusoidal voltage is the one normally expected in this type of DC/AC conversion.

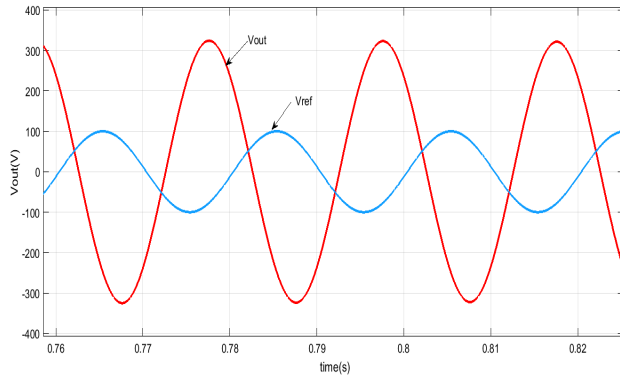


Fig.14 Terminal voltage of the load.

L. Evolution of the Voltage Harmonic Distortion Rate

It can be seen that, apart from the system start-up phase, the overall voltage harmonic distortion rate is 0,41% THD, which is acceptable according to the EN50160 standard

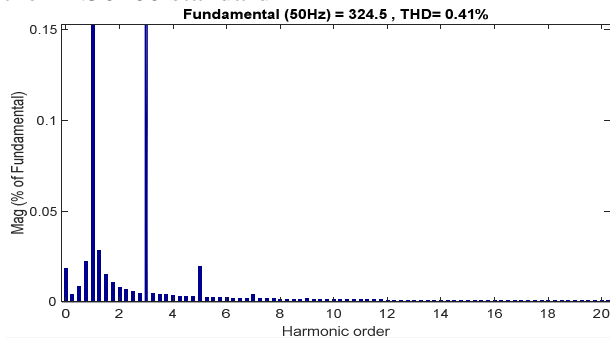


Fig.15. Harmonic spectrum of the voltage across the load

M. Current in the Load and Voltage at the load terminals

For several values of load impedance: 150Ω, 250Ω, 350Ω, it can be seen that the inrush current varies according to the value of the load resistance or impedance while the voltage is fixed at the maximum value of 325V and frequency 50Hz.

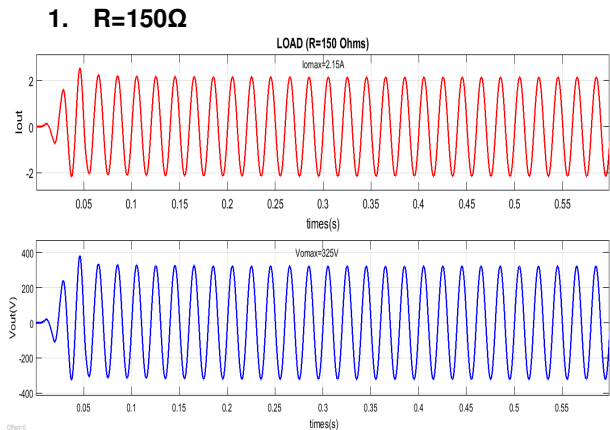


Fig.16.1 Current and Terminal voltage of the load.

2. R=250Ω

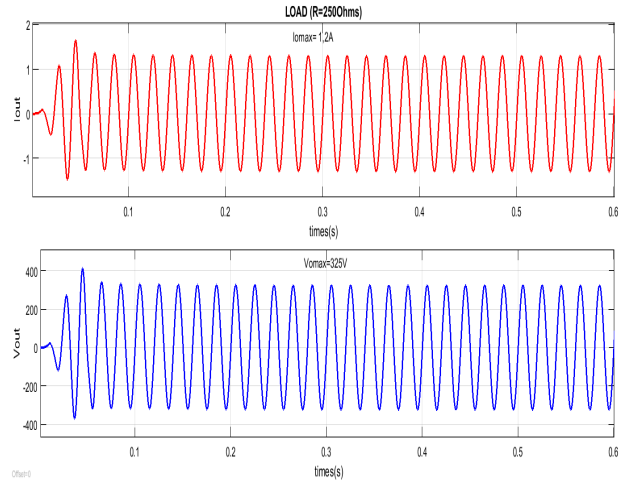


Fig.16.2 Current and Terminal voltage of the load.

3. R=350Ω

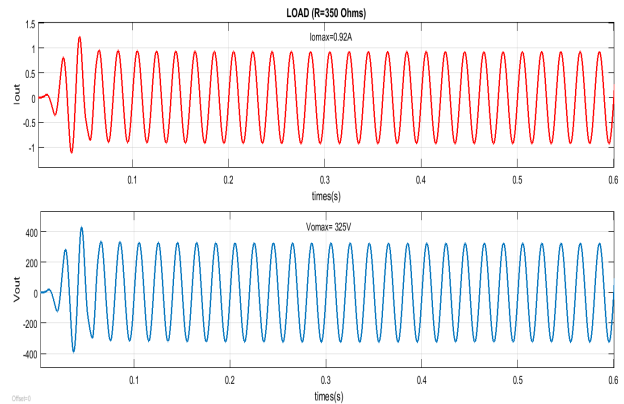


Fig.16.3 Current and Terminal voltage of the load.

N. Current Harmonic Distortion Rate

It can be seen that the current harmonic distortion rate for each value of the load is also less than 0,50%. Acceptable THD according to EN50160

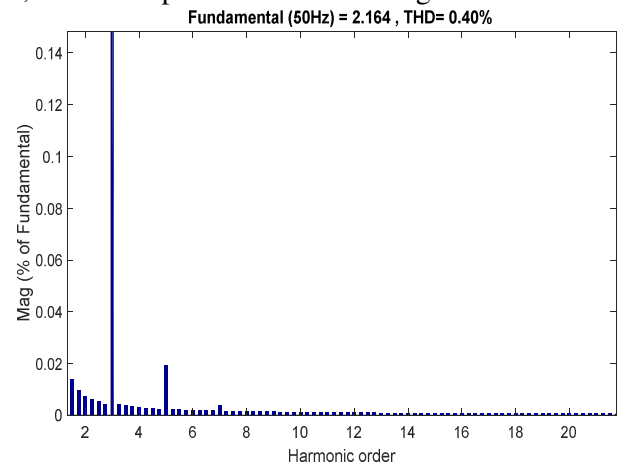


Fig.17. Harmonic spectrum of the current in the load R=150Ω.

IV. CONCLUSION

This paper presents a new sinusoidal duty cycle modulation, control principle for single-phase PV stand-alone inverters in closed-loop. The general architecture, states model modeling, and simulation of the new PV stand-alone inverter prototype are presented as well as the virtual simulation results for several values of load resistance in the Matlab/Simulink platform. It can be seen that despite the variations of the load resistance, the voltage at its terminal remains constant in amplitude, profile, frequency and is equal to the previously defined reference; it does not change with the variation of the load resistance as it was the case in open loop.

REFERENCES

- [1] Matina Lakka, Eftichios Koutroulis, Member, IEEE, and Apostolos Dollas, Senior Member, IEEE «Development of an FPGA-Based SPWM Generator for High Switching Frequency DC/AC Inverters» IEEE Transactions On power Electronics, vol. 29, no. 1, january 2014.
- [2] Heinz Willi, Hans-Christoph, Member,IEEE,And Georg Viktor Stanke« Analysis and Realization of a Pulse width Modulator Based on Voltage -Space Vectors» IEEE Transactions on Industry Applications, vol 24. No 1. January/february 1988.
- [3] Baojian Ji, Jianhua Wang, Member, IEEE, and Jianfeng Zhao « High-Efficiency Single-Phase Transformerless PV H6 Inverter With Hybrid Modulation Method » IEEE Transactions On Industrial Electronics, Vol. 60, no. 5, May 2013.
- [4] Amirhossein Moeini, Hossein Iman-Eini, Mohamadkazem Bakhshizadeh « Selective harmonic mitigation-pulse-width modulation technique with variable DC-link voltages in single and three-phase cascaded H-bridge inverters » IET Power Electronics · April 2014.
- [5] B. Ismail, S.Taib MIEEE, A. R Mohd Saad, M. Isa, C. M. Hadzler «Development of a Single Phase SPWM Microcontroller-Based Inverter» First International Power and Energy Conference PECon 2006 November 28-29, 2006.
- [6] Jean Mbihi, "Informatique et automation: Automatismes programmables contrôlés par ordinateur", pp. 103-113, Editons Publibook, 2005.
- [7] J. Mbihi, B. Ndjali, and M. Mbouenda, "Modelling and simulation of a class of duty cycle modulators for industrial instrumentation", Iranian Journal of Electrical and Computer Engineering, vol.4, N°2, pp. 121-128, 2005.
- [8] J. Mbihi, F. Ndjali Beng, M. Kom, and L. Nneme Nneme, "A novel analog-to-digital conversion technique using non linear duty-cycle modulation", International Journal of Electronics and Computer Science Engineering, Volume 1, Number 3, pp. 818-825, 2012.
- [9] J. Mbihi, L. Nneme Nneme, "A multi-channel analog-to-digital conversion technique using parallel duty-cycle modulation", International Journal of Electronics and Computer Science Engineering, Volume 1, Number 3, pp. 826-833, 2012.
- [10] B. Moffo Lonla, J. Mbihi, L. Nneme Nneme, and M. Kom, "A novel digital-to-analog Conversion technique using duty-cycle modulation", International Journal of Circuits, Systems and Signal Processing, Issue 1, Vol. 7, pp. 42-49, 2013
- [11] B. Moffo Lonla, J. Mbihi, L. Nneme Nneme, and M. Kom, "A Low Cost and High Quality Duty-Cycle Modulation Scheme and Applications", International Journal of Electrical, Computer, Energetic, Electronic and Communication Engineering Vol:8, No:3, 2014.
- [12] L. N. Nneme, B. M. Lonla and J. Mbihi « Review of a Multipurpose Duty-Cycle Modulation Technology in Electrical and Electronics Engineering », p. 10.
- [13] J. Mbihi, L. Nneme Nneme "virtual simulation and comparison of sine pulse zidhand sine duty cycle modulation drivers for single phase power inverters", JEECCS,Volume 6,Issue 21,pages 31-38,2020.
- [14] M.J.P.Pesdjock, J.R.M.Pone, D.Tchiotsop, M.R.Douanla, G. Kenne "minimization of currents harmonics injected for grid connected photovoltaic system using duty cycle modulation technique", International Journal of dynamic and control, 31 October 2020.
- [15] A. O. Biyobo, L. N. Nneme, et J. Mbihi, « A Novel Sine Duty-Cycle Modulation Control Scheme for Photovoltaic Single-Phase Power Inverters », vol. 17, p. 9, 2018.
- [16] P. O. Etouke, L. N. Nneme, J. Mbihi « An Optimal Control Scheme for a Class of Duty-Cycle Modulation Buck Choppers: Analog Design and Virtual Simulation », Journal of Electrical Engineering, Electronics, Control and Computer Science –JEECCS, Volume 6, Issue 19, pages 13-20, 2020
- [17] Y. P. Dangwe Sounsoumo, Jean Mbihi, Haman-djalo and Joseph Yves Effa, "Virtual Digital Control Scheme for a Duty-Cycle Modulation Boost Converter ", Journal of Computer Science and Control Systems, Volume 10, No 2, pp. 22-27, October 2017, Romania.
- [18] Y. P. Dangwe Sounsoumo, Haman DJALO, Jean Mbihi et J. Y. EFFA , " Modélisation et simulation virtuelle d'un nouveau schéma de réglage de hacheurs Boost à commande rapprochée par modulation en rapport cyclique ", Journal Afrique Science , pp. 176-185, Vol. 13, No. 1, 2017, Côte d'Ivoire, <http://www.afriquescience.info>.
- [19] J. Mbihi, L. Nneme Nneme, "A novel Control Scheme for Buck Power Converters using Duty-Cycle Modulation", International Journal of Power Electronics, Vol. 5, N°3/4, pp 185 - 199, October 2013, Switzerlan..
- [20] Nguéack Tatou Laurel, Paune Felix, Kenfack W. Gutenberg, Mbihi Jean «A Novel Optical Fiber Transmission System Using Duty-Cycle Modulation and Application to ECG Signal: Analog Design and Simulation » Journal of Electrical Engineering, Electronics, Control and Computer Science – JEECCS, Volume 6, Issue 21, pages 39-48, 2020.
- [21] Otam Steve Ulriche, Moffo Lonla Bertrand, Gamom Ngounou E. R. Christian, Mbihi Jean « A novel FPGA-Based Multi-Channel Signal Acquisition System Using Parallel Duty-Cycle Modulation and Application to Biologic Signals: Design and Simulation » Journal of Electrical Engineering, Electronics, Control and Computer Science –JEECCS, Volume 7, Issue 24, pages 13-20, 2021
- [22] Wend-Waoga Anthelme ZEMANE « Amelioration De La Duree De Vie Du Condensateur Sur Le Bus Cc De L'onduleur Pour L'application Photovoltaïque » Montréal 2015.
- [23] Muhammad H.Rachid « Power Electronics, circuits, devices, and applications», Prentice Hall, Englewood CM s, New Jersey 1993.
- [24] SPIROV Dimitar, LAZAROV Vladimir, ROYE Daniel†, ZARKOV Zahari, MANSOURI Omar† « Modelisation Des Convertisseurs Statiques DC-DC Pour Des Applications Dans Les Energies Renouvelables En Utilisant Matlab/Simulink » Université Technique de Sofia, 8 Kliment Ohridski, Sofia 1000, Bulgarie †G2ELab, UMR 5269 INPG-UJF-CNRS, ENSIEG - BP 46 – 38402.
- [25] Heng DENG, Ramesh ORUGANTI, Dipti SRINIVASA Centre for Power Electronics, Dept of Electrical and Computer Engineering National University of Singapore, Singapore, « Modeling and Control of Single-Phase UPS Inverters » IEEE PEDS 2005.
- [26] L. O. Aghenta and M. Tariq Iqbal « Design and Dynamic Modelling of a Hybrid Power System for a House in Nigeria » International Journal of Photoenergy, Volume 2019.